BLIND AND ROBUST MESH WATERMARKING USING MANIFOLD HARMONICS

Kai Wang[1]*, Ming Luo*[2]*, Adrian G. Bors*[2]*, and Florence Denis*[3]

[1] Université de Lyon, CNRS, INSA-Lyon, LIRIS, UMR5205, F-69621, France
[2] Department of Computer Science, University of York, York YO10 5DD, UK
[3] Université de Lyon, CNRS, Université Lyon 1, LIRIS, UMR5205, F-69622, France

ABSTRACT

In this paper, we present a new blind and robust 3-D mesh watermarking scheme that makes use of the recently proposed manifold harmonics analysis. The mesh spectrum coefficient amplitudes obtained by using this analysis are quite robust against various attacks, including connectivity changes. A blind 16-bit watermark is embedded through an iterative scalar Costa quantization of the low frequency coefficient amplitudes. The imperceptibility of the watermark is ensured since the human visual system has been proved insensitive to the mesh low frequency components modification. The embedded watermark is experimentally robust against both geometry and connectivity attacks. Comparison results with two state-of-the-art methods are provided.

Index Terms— Mesh watermarking, blind, manifold harmonics

1. INTRODUCTION

The robust and blind watermarking technique seems an efficient solution to the emerging problem of intellectual property protection of 3-D meshes. Such watermarking methods do not need the original cover mesh for the watermark extraction and are resistant against various attacks on the stego model. In general, devising a robust and blind mesh watermarking scheme is a difficult task, mainly due to the mesh's irregular representation and the existence of many intractable attacks [1]. Some spatial methods [2, 3] use statistical mesh shape descriptors as watermarking primitives and achieve both robustness and blindness. For example, in [3], the distribution of the mesh vertex norms is modified to hide a multi-bit watermark. This approach has been considered as the most robust blind scheme proposed so far. Watermarking in the mesh spectral domain has the advantages of being more secure and more imperceptible mainly due to the spreading effect of the embedded watermark in all the spatial parts of the stego model. However, most existing spectral methods are non-blind [4, 5] since they use combinatorial Laplacian spectral analysis [6] which is not robust against connectivity changes. Blindness in the spectral domain was first exploited in [7]. Two recently proposed blind spectral methods [8, 9] have achieved a better robustness, especially against connectivity attacks (e.g. surface simplification and remeshing). In [8], the robustness relies on the stability of the constraints embedded in sets of high frequency coefficients. Unlike the other spectral schemes, the method of Liu *et al.* [9] makes use of a new mesh spectrum decomposition tool, namely the manifold harmonics analysis [10]. The manifold harmonics spectrum coefficients are quite robust, even after connectivity alterations. In Liu's method, the low frequency part of the mesh spectrum is split into 5 slots. One bit is inserted in each slot by modifying the relative relationship between the magnitude of a certain selected coefficient and the average magnitude of the other coefficients in the slot.

Our objective in this paper is to use the quantization-based data hiding technique to embed a blind and robust watermark in the manifold harmonics spectral domain of a 3-D mesh. We would like to improve the achievable watermarking capacity in this promising domain (currently 5 bits as in the scheme of Liu *et al.* [9]), while preserving as well as possible the other performance metrics (i.e. security, robustness and imperceptibility). In our scheme, a multi-bit watermark is embedded through an iterative quantization of the low frequency coefficients obtained by means of the manifold harmonics analysis. The security is enhanced since the watermark is spread to all the spatial parts of the stego mesh, with a low possibility to introduce predictable spatial patterns on the mesh surface. Therefore, it is even difficult to notice its existence. A satisfactory robustness can be achieved because the low frequency information is perceptually important, and thus is less likely to be changed under attacks. It has also been shown that the human visual system is not sensitive to the low frequency component modifications of a 3-D mesh [11]. This means that we can also achieve a good watermark imperceptibility.

The remainder of this paper is organized as follows: the manifold harmonics analysis is introduced in Section 2; the proposed watermark embedding and extraction algorithms are detailed in Section 3; in Section 4, some experimental results are presented, with comparisons with the methods of Cho *et al.* [3] and Liu *et al.* [9]; we draw the conclusions in Section 5.

2. MANIFOLD HARMONICS ANALYSIS

In this section, we briefly introduce the manifold harmonics analysis. Readers could refer to [10] for more details. Similar to the Laplace operator in Euclidean space, the Laplace-Beltrami operator Δ is defined as the divergence of the gradient for functions defined over a manifold $\mathscr{S}$ with metric tensor g:

$$\Delta = \operatorname{div}\operatorname{grad} = \sum_{i,j} \frac{1}{\sqrt{|g|}} \frac{\partial}{\partial \xi_i} \left(\sqrt{|g|} g^{i,j} \frac{\partial}{\partial \xi_j} \right), \qquad (1)$$

where $|g|$ denotes the determinant of g, and $g^{i,j}$ are the components of the inverse of g. The eigenfunction and eigenvalue pairs $\left(H^k, \lambda_k\right)$ of the operator Δ on $\mathscr{S}$ satisfy the following relationship:

$$-\Delta H^k = \lambda_k H^k. \qquad (2)$$

The above eigen-problem is then discretized and simplified within the finite element modeling framework on the n vertices $v_{i,i=1,2,\ldots,n}$ of the surface $\mathscr{S}$. This yields the following matrix formulation:

$$-Q\mathbf{h}^k = \lambda_k D\mathbf{h}^k, \qquad (3)$$

This work is in part supported by China Scholarship Council of the Chinese government and by the French National Research Agency (ANR) through Collaviz project (ANR-08-COSI-003-12).

where $\mathbf{h}^k = \left[H_1^k, H_2^k, ..., H_n^k\right]^T$, the $n \times n$ matrix D is diagonal and called the lumped mass matrix with $D_{i,i} = \left(\sum_{t \in \mathcal{N}_t(i)} |t|\right)/3$, and Q is also of size $n \times n$ and called the stiffness matrix with

$$\begin{cases} Q_{i,j} = \left(\cot(\beta_{i,j}) + \cot(\beta_{i,j}^{'})\right)/2, \\ Q_{i,i} = -\sum_j Q_{i,j}. \end{cases} \tag{4}$$

In the above expressions, $\mathcal{N}_t(i)$ denotes the set of triangles incident to vertex v_i, $|.|$ gives the area of a triangle, and $\beta_{i,j}, \beta_{i,j}^{'}$ are the two angles opposite to the edge that connects v_i and v_j. The eigenvectors solutions of Eq. (3) are the manifold harmonics bases, while the eigenvalues represent their associated frequencies. The bases are orthogonal with regard to the functional inner product. We then sort the bases according to the ascending order of their associated frequencies and also scale them so that they have unit norms. The spectral coefficients are calculated as the functional inner product between the geometry $\mathbf{x}$ (resp. $\mathbf{y}, \mathbf{z}$) and the sorted and orthonormal bases:

$$\tilde{x}_k = \left\langle \mathbf{x}, \mathbf{h}^k \right\rangle = \sum_{i=1}^{n} x_i D_{i,i} H_i^k. \tag{5}$$

Finally, the k-th spectral coefficient amplitude is defined as:

$$c_k = \sqrt{(\tilde{x}_k)^2 + (\tilde{y}_k)^2 + (\tilde{z}_k)^2}. \tag{6}$$

The object can be exactly reconstructed by using the inverse manifold harmonics transform. For geometry $\mathbf{x}$ (resp. $\mathbf{y}, \mathbf{z}$), we have

$$x_i = \sum_{k=1}^{n} \tilde{x}_k H_i^k. \tag{7}$$

The first few low frequency coefficients can be efficiently calculated by using the band-by-band algorithm combined with an efficient eigen-solver such as TAUCS or SuperLU [10]. For instance, the first 100 coefficients of the Rabbit mesh having about 33.5K vertices can be obtained in less than 40 seconds on an ordinary PC.

3. WATERMARK EMBEDDING AND EXTRACTION

Our watermark embedding method is composed of three main steps: (a) carry out the mesh spectrum decomposition by using Eq. (5) with the mesh's manifold harmonics bases; (b) quantize the amplitudes of some low frequency coefficients c_k to hide a 16-bit watermark $w_{j,j=1,2,...,16}$, by using the 2-symbol scalar Costa scheme [12]; (c) reconstruct the watermarked mesh with the modified coefficients using Eq. (7).

In step (b), for each c_k that is to be watermarked, a structured pseudo-random codebook is given by:

$$\mathcal{U}_{c_k, t_{c_k}} = \bigcup_{l=0}^{1} \left\{ u = zS + l\frac{S}{2} + t_{c_k} S, u \geq 0 \right\}, \tag{8}$$

where z is an integer, S is the quantization step, $l \in \{0, 1\}$ is the watermark bit from the codeword u, and t_{c_k} is a pseudo-random sequence generated by using a secret key K. As an example, t_{c_k} can be uniformly distributed in $\left[-\frac{1}{2}, \frac{1}{2}\right]$. The dither signal $t_{c_k} S$ is introduced to further enhance the watermarking security. Note that the codewords in $\mathcal{U}_{c_k, t_{c_k}}$ represent bits of 0 and 1 in an interleaved manner. In order to insert a watermark bit w^{c_k} in c_k, we first find the nearest codeword u_{c_k} to c_k in the codebook that correctly represents w^{c_k}. This means w^{c_k} should be equal to value l in the derivation of u_{c_k} given in Eq. (8). Then, the quantized value $c_k^{'}$ is calculated as:

$$c_k^{'} = c_k + \alpha\left(u_{c_k} - c_k\right), \tag{9}$$

where $\alpha \in [0, 1]$ represents the distortion compensation factor. The proposed bit embedding procedure consists in pushing c_k towards u_{c_k}, to within the interval $\left(u_{c_k} - \frac{S}{4}, u_{c_k} + \frac{S}{4}\right)$, which is the decoding area of u_{c_k} under the nearest neighbor criterion. Finally, the modified spectral coefficients $\tilde{x}_k^{'}$ (resp. $\tilde{y}_k^{'}, \tilde{z}_k^{'}$) can be obtained as:

$$\tilde{x}_k^{'} = \frac{c_k^{'}}{c_k} \tilde{x}_k. \tag{10}$$

The quantization mechanism is quite simple, but there are still some important details about the whole watermark embedding algorithm. Actually, two issues have to be carefully taken into account during its design: the causality problem and the invariance to similarity transformation.

First, it can be noticed that once we modify the spectral coefficients of a model from $\tilde{x}_k, \tilde{y}_k, \tilde{z}_k$ to $\tilde{x}_k^{'}, \tilde{y}_k^{'}, \tilde{z}_k^{'}$ and reconstruct the deformed object, the manifold harmonics bases of the reconstructed object are different from those of the original model. It means that after the re-decomposition of the deformed object, the obtained coefficients, denoted by $\tilde{x}_k^{''}, \tilde{y}_k^{''}, \tilde{z}_k^{''}$, are different from the desired values $\tilde{x}_k^{'}, \tilde{y}_k^{'}, \tilde{z}_k^{'}$. One way to solve this causality problem is to repetitively perform the quantization, in a similar way to [9]. The previously watermarked mesh is input to the watermark embedding system with its spectrum coefficients re-quantized. This process is carried out for several iterations, until all the bits are correctly embedded. In order to reduce the number of iterations, we take the following measures. First, we do not quantize the first 20 coefficients. Experimentally, modifying them will also cause noticeable alterations of the subsequent coefficients and thus increase the processing time. Second, starting from c_{21}, we quantize every 3 out of 4 amplitudes. This creates some "buffering space" between watermarking primitives, which can effectively alleviate the causality problem. Even after taking the above two measures, sometimes we still need a large number of iterations until all the 16 primitive amplitudes are correctly quantized. Therefore, we introduce the third measure: trying to repetitively embed the 16 bits for 3 times. This repetition is capable of reducing the processing time even though we now have more amplitudes to quantize. Actually, the 16 bits are considered successfully embedded as long as the majority voting results from the corresponding repetitively embedded bits are correct. The iterative procedure can then be terminated earlier, even when there still exist embedding errors on certain "difficult" amplitudes.

Similarity transformation includes translation, rotation and uniform scaling. It can be deduced that under translation, only the first manifold harmonics base $\mathbf{h}^1$ is altered. Since the first spectral amplitude c_1 is not involved in watermarking, our method is immune to translation. Meanwhile, the manifold harmonics bases are kept unchanged under isometric transformation; thus, a rotation in the spatial domain x, y, z yields the same rotation in the spectral domain $\tilde{x}_k, \tilde{y}_k, \tilde{z}_k$, without any influence on the coefficient amplitudes c_k. It can be proved that under a uniform scaling with a factor s, all the spectral coefficients will be scaled by s^2. In order to be immune to scaling, we determine the quantization step of c_k as $S = \beta c_2$, with β a constant. In this way, the codewords in Eq. (8) change proportionally with c_k under uniform scaling so the invariance is ensured. Experimentally, β can be fixed as 0.0015 for all the objects without seriously affecting the algorithm's performance.

Algorithm 1 summarizes the whole watermark embedding procedure. The first 15 steps constitute the watermark extraction algorithm. If the embedding algorithm is terminated within few iterations, the procedure can be further continued while neglecting the stop criterion at step 16, in order to get another one or two stego-models, which probably have smaller err_2 value (see step 15 for its calculation) but higher induced distortion. Then, we can select one from them as the final watermarked model according to the re-

quired trade-off between the distortion and the robustness. Normally, a model with a smaller err_2 value possesses a stronger robustness.

Algorithm 1 Watermark embedding algorithm.

1: Calculate the first 84 spectral coefficients and their amplitudes c_k of the input mesh by using the manifold harmonics analysis;
2: Record the difference part of the mesh geometry as $\bar{x}_i = x_i - \sum_{k=1}^{84} \tilde{x}_k H_i^k$ (resp. $\bar{y}_i, \bar{z}_i$);
3: Initialization: $k = 21, j = 1$;
4: **while** $k \leq 84$ **do**
5: **if** $k\%4 \neq 0$ (not being "buffering space") **then**
6: Construct the codebook $\mathcal{U}_{c_k,t_{c_k}}$ for c_k according to Eq. (8) with the quantization step $S = \beta c_2$;
7: Find the nearest codeword u_{c_k} in $\mathcal{U}_{c_k,t_{c_k}}$ to c_k, and record the embedded bit of u_{c_k} as $\tilde{w}_j$;
8: $j \leftarrow j + 1$;
9: **end if**
10: $k \leftarrow k + 1$;
11: **end while**
12: **for** $j = 1$ to 16 **do**
13: Deduce the extracted bit $\hat{w}_j$ through majority voting between $\tilde{w}_j, \tilde{w}_{j+16}, \tilde{w}_{j+32}$;
14: **end for**
15: Compare with $w_{j,j=1,2,\ldots,16}$ and its periodic extension $w_{j,j=1,2,\ldots,48}$ (for $j > 16$ we have $w_j = w_{(j\%16)}$), count the bit error number of $\hat{w}_{j,j=1,2,\ldots,16}$ as err_1 and the bit error number of $\tilde{w}_{j,j=1,2,\ldots,48}$ as err_2;
16: **if** $(err_1 == 0)$ AND $(err_2 < 6)$ **then**
17: Stop iterations, take the current mesh as watermarked model;
18: **else**
19: Initialization: $k = 21, j = 1$;
20: **while** $k \leq 84$ **do**
21: **if** $k\%4 \neq 0$ **then**
22: Deduce the to-be-embedded bit of c_k as $w_{(j\%16)}$;
23: Calculate the quantized value $c_k^{'}$ by using the 2-symbol scalar Costa scheme with quantization step $S = \beta c_2$;
24: Obtain the modified spectral coefficients $\tilde{x}_k^{'}, \tilde{y}_k^{'}, \tilde{z}_k^{'}$ by using Eq. (10);
25: $j \leftarrow j + 1$;
26: **end if**
27: $k \leftarrow k + 1$;
28: **end while**
29: **end if**
30: Reconstruct the deformed mesh geometry with $x_i^{'} = \bar{x}_i + \sum_{k=1}^{84} \tilde{x}_k^{'} H_i^k$ (resp. $y_i^{'}, z_i^{'}$);
31: Return to step 1 with the reconstructed model as input.

4. EXPERIMENTAL RESULTS

The proposed method has been tested on several meshes such as: Rabbit (33520 vertices), Horse (36043 vertices) and Venus (67173 vertices). Table 1 details some statistics about the watermark embedding and extraction. These values represent averages of 5 trials with 5 different watermark codes. In the parentheses are the corresponding results of the Method I of Cho *et al.* [3] with the strength factor equal to 0.025 and with the same capacity 16 bits. All the tests were carried out on a Pentium IV 2.0GHz processor with 2GB memory. It can be seen that our approach can be successfully applied on relatively large datasets with acceptable embedding and extraction times. The objective distortion between the watermarked and original meshes is measured by Metro [13] in terms of maximum root mean square error (MRMS). A "perceptual" distance between them is evaluated by the mesh structural distortion measure (MSDM) proposed in [14] (radius equal to 0.005). Its value tends towards 1 (theoretical limit) when the measured objects are visually very different and is equal to 0 for identical ones. One advantage of our method is that it can introduce relatively high-amplitude deformation while keeping it imperceptible. This point has also been confirmed in Fig. 1, where the original and watermarked Horses are illustrated. We can hardly observe any visual difference between them.

Table 1. Baseline evaluations of the proposed method (16 bits capacity, in the parentheses are the results of Cho's method).

Model	Rabbit	Horse	Venus
Iteration number	12.2	13.4	8.6
Embedding time (s)	316.6 (1.5)	278.0 (1.6)	521.0 (2.4)
Extraction time (s)	23.5 (<1.0)	20.1 (<1.0)	52.9 (<1.0)
MRMS by WM (10^{-3})	2.37 (2.14)	2.37 (1.57)	1.95 (1.19)
MSDM by WM	0.17 (0.20)	0.13 (0.21)	0.13 (0.21)

Table 2. Robustness evaluation results in terms of BDR (16 bits capacity, in the parentheses are the results of Cho's method).

Noise	0.10%	0.20%	0.30%	0.40%	0.50%
Rabbit	1 (1)	0.99 (1)	0.99 (0.96)	0.93 (0.94)	0.81 (0.93)
Horse	0.98 (1)	0.96 (0.98)	0.89 (1)	0.80 (0.99)	0.74 (0.96)
Venus	1 (1)	0.99 (0.93)	0.96 (0.91)	0.79 (0.88)	0.79 (0.84)
Smooth.	10-itera.	20-itera.	30-itera.	40-itera.	50-itera.
Rabbit	0.98 (0.98)	0.94 (0.96)	0.91 (0.93)	0.93 (0.90)	0.88 (0.90)
Horse	0.90 (1)	0.81 (0.99)	0.70 (0.99)	0.63 (0.98)	0.59 (0.94)
Venus	0.99 (0.96)	0.95 (0.89)	0.89 (0.83)	0.83 (0.79)	0.79 (0.71)
Simplif.	10%	30%	50%	70%	90%
Rabbit	1 (0.98)	0.99 (0.90)	0.94 (0.76)	0.90 (0.71)	0.68 (0.64)
Horse	0.99 (0.91)	0.93 (0.48)	0.84 (0.81)	0.58 (0.63)	0.53 (0.71)
Venus	1 (0.91)	0.98 (0.90)	0.99 (0.88)	0.81 (0.79)	0.51 (0.64)

The robustness of both schemes has been tested under noise addition, Laplacian smoothing (deformation factor equal to 0.03) and surface simplification through vertex reduction. The robustness is evaluated in terms of watermark bit detection ratio (BDR), defined as the ratio of the correctly extracted bits. Table 2 presents the robustness evaluation results of both methods (those of Cho's method are in parentheses), which are also the averages of 5 trials. Our method is quite robust against various attacks, as long as they do not significantly modify the shape of the mesh. However, the results are not that good on Horse. For this object we guess that the manifold harmonics bases may be sensitive to the deformation of the obtrusive parts of this model (e.g. the ears and the feet) under attacks.

Under the current parameter setting, the two methods show comparable robustness against various attacks, except for extremely strong ones, against which Cho's method is more resistant. More precisely, it seems that our method works better for mesh simplification while Cho's method performs better for noise addition and smoothing. Under this comparable robustness precondition, the watermarked models of Cho's method have lower objective distortion, while ours have a higher visual quality. Actually, Cho's method is prone to introduce some ring-like high-frequency distortions to the watermarked meshes, especially on smooth parts like the cheek of Venus (see Fig. 2.(a)). Contrarily, the distortion induced by our

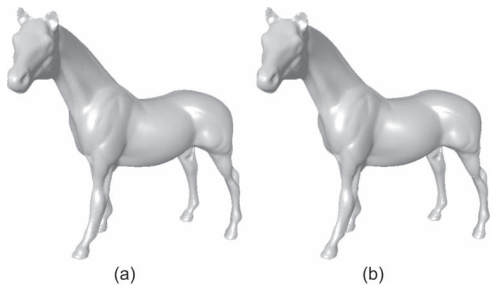

Fig. 1. (a) Original Horse; (b) Watermarked Horse by our method.

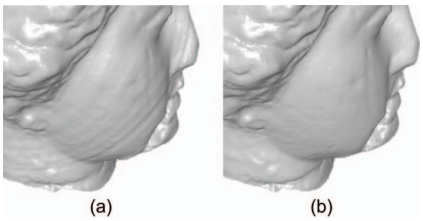

Fig. 2. Watermark imperceptibility comparison: (a) Venus watermarked by Cho's method; (b) Venus watermarked by our method.

Table 3. Baseline evaluations of the proposed method (5 bits capacity, in the parentheses are the results of Liu's method).

Model	Rabbit	Horse	Venus
Iteration number	7.3 (6.0)	6.7 (8.3)	4.7 (5.7)
Embedding time (s)	139.6 (116.6)	107.6 (140.0)	208.7 (250.6)
Extraction time (s)	18.2 (18.9)	15.4 (16.1)	43.2 (43.4)
MRMS by WM (10^{-3})	1.50 (3.32)	1.43 (4.42)	1.14 (2.72)
MSDM by WM	0.11 (0.20)	0.09 (0.20)	0.09 (0.12)

method is of low frequency and it is difficult for the human eyes to perceive it (see Fig. 2.(b)). In all, we can conclude that the better imperceptibility of our spectral method compensates the higher computational demand when compared to Cho's spatial method.

In the following, we compare the proposed method with the scheme of Liu *et al.* [9], which is also based on the manifold harmonics analysis but with a capacity of 5 bits. In order to perform a fair comparison between the two schemes, we have slightly modified our method so as to ensure the premise of a same watermarking capacity. More precisely, 5 bits are embedded repetitively for 5 times from the 21st to the 70th spectral amplitudes (therefore we quantize every one out of two amplitudes). Meanwhile, in Liu's algorithm, the 21st to the 70th amplitudes are divided into 5 slots and one bit is embedded in each slot. The parameters of these two algorithms are chosen so that they have roughly a comparable overall robustness performance. For Liu's method, we use the option of normal slot combined with non-aggressive embedding so as to introduce less distortion (the parameter s in their algorithm is fixed as 0.20).

Table 3 presents the comparison results concerning the execution times and the induced distortion, and Table 4 presents the robustness evaluation results of the two algorithms, also in terms of BDR. In both tables, the results of Liu's method are presented in parentheses and all the values are the averages of 3 trials. It can be seen that with a roughly comparable robustness level, our method introduces lower geometric and perceptual distortions than Liu's method. This implies that our watermarking scheme has a better trade-off between the robustness and the induced distortion.

5. CONCLUSION AND FUTURE WORK

A new blind and robust spectral mesh watermarking method has been proposed in this paper. A multi-bit watermark is embedded in a mesh by iteratively quantizing its low frequency spectral amplitudes obtained after a manifold harmonics transform. The main features of our method are its high imperceptibility and security, its good robustness against connectivity attacks as well as its applicability on relatively large meshes. However, our method may fail for certain objects: either the model's manifold harmonics spectral coefficients are not that robust, or it is impossible to correctly embed the watermark, even after many iterations. It would be interesting to investigate the reasons for these two shortcomings. We are also interested in improving the watermark robustness and capacity, and in devising an efficient and elegant way to solve the causality problem.

Table 4. Robustness evaluation results in terms of BDR (5 bits capacity, in the parentheses are the results of Liu's method).

Noise	0.10%	0.20%	0.30%	0.40%	0.50%
Rabbit	1 (1)	1 (1)	0.93 (0.93)	0.87 (0.87)	0.93 (0.93)
Horse	1 (1)	0.93 (0.87)	0.93 (0.93)	0.93 (0.93)	0.73 (0.73)
Venus	1 (1)	0.93 (0.93)	0.87 (0.87)	0.73 (0.80)	0.80 (0.80)
Smooth.	10-itera.	20-itera.	30-itera.	40-itera.	50-itera.
Rabbit	1 (0.80)	1 (0.73)	1 (0.67)	1 (0.60)	0.93 (0.60)
Horse	1 (0.93)	0.93 (0.87)	0.73 (0.80)	0.67 (0.80)	0.63 (0.80)
Venus	1 (0.80)	1 (0.80)	1 (0.80)	0.87 (0.80)	0.73 (0.73)
Simplif.	10%	30%	50%	70%	90%
Rabbit	1 (1)	1 (1)	1 (0.93)	1 (0.87)	0.73 (0.67)
Horse	1 (1)	1 (0.80)	0.93 (0.73)	0.93 (0.73)	0.40 (0.73)
Venus	1 (1)	1 (1)	1 (1)	1 (0.93)	0.93 (0.73)

6. REFERENCES

[1] K. Wang, G. Lavoué, F. Denis, and A. Baskurt, "A comprehensive survey on three-dimensional mesh watermarking," *IEEE Trans. on Multimedia*, vol. 10, no. 8, pp. 1513–1527, 2008.

[2] S. Zafeiriou, A. Tefas, and I. Pitas, "Blind robust watermarking schemes for copyright protection of 3D mesh objects," *IEEE Trans. on Vis. and Comput. Graphics*, vol. 11, no. 5, pp. 596–607, 2005.

[3] J.-W. Cho, R. Prost, and H.-Y. Jung, "An oblivious watermarking for 3D polygonal meshes using distribution of vertex norms," *IEEE Trans. on Signal Process.*, vol. 55, no. 1, pp. 142–155, 2007.

[4] R. Ohbuchi, A. Mukaiyama, and S. Takahashi, "A frequency-domain approach to watermarking 3D shapes," *Comput. Graphics Forum*, vol. 21, no. 3, pp. 373–382, 2002.

[5] G. Lavoué, F. Denis, and F. Dupont, "Subdivision surface watermarking," *Comput. & Graphics*, vol. 31, no. 3, pp. 480–492, 2007.

[6] Z. Karni and C. Gotsman, "Spectral compression of mesh geometry," in *Proc. ACM SIGGRAPH*, 2000, pp. 279–286.

[7] F. Cayre, P. R. Alface, F. Schmitt, B. Macq, and H. Maître, "Application of spectral decomposition to compression and watermarking of 3D triangle mesh geometry," *Signal Process.: Image Commun.*, vol. 18, no. 4, pp. 309–319, 2003.

[8] M. Luo and A. G. Bors, "Principal component analysis of spectral coefficients for mesh watermarking," in *Proc. IEEE Int. Conf. on Image Process.*, 2008, pp. 441–444.

[9] Y. Liu, B. Prabhakaran, and X. Guo, "A robust spectral approach for blind watermarking of manifold surfaces," in *Proc. ACM Workshop on Multimedia and Security*, 2008, pp. 43–52.

[10] B. Vallet and B. Lévy, "Spectral geometry processing with manifold harmonics," *Comput. Graphics Forum*, vol. 27, no. 2, pp. 251–260, 2008.

[11] O. Sorkine, D. Cohen-Or, and S. Toledo, "High-pass quantization for mesh encoding," in *Proc. Symp. on Geometry Process.*, 2003, pp. 42–51.

[12] J. J. Eggers, R. Bauml, R. Tzschoppe, and B. Girod, "Scalar costa scheme for information embedding," *IEEE Trans. on Signal Process.*, vol. 51, no. 4, pp. 1003–1019, 2003.

[13] P. Cignoni, C. Rocchini, and R. Scopigno, "Metro: Measuring error on simplified surfaces," *Comput. Graphics Forum*, vol. 17, no. 2, pp. 167–174, 1998.

[14] G. Lavoué, E. D. Gelasca, F. Dupont, A. Baskurt, and T. Ebrahimi, "Perceptually driven 3D distance metrics with application to watermarking," in *Proc. SPIE Electronic Imaging*, 2006, vol. 6312, pp. 63120L.1–63120L.12.